Fluorescence Imaging of Bacterial Killing by Antimicrobial Peptide Dendrimer G3KL

*Bee-Ha Gan, Thissa N. Siriwardena, Sacha Javor, Tamis Darbre and Jean-Louis Reymond**

[a] *Department of Chemistry and Biochemistry, University of Bern, Freiestrasse 3, 3012 Bern, Switzerland. e-mail: jean-louis.reymond@dcb.unibe.ch*

Abstract: we recently discovered that peptide dendrimers such as **G3KL** ((KL)$_8$(*K*KL)$_4$(*K*KL)$_2$*K*KL, *K* = branching L-lysine) exert strong activity against Gram-negative bacteria including *Pseudomonas aeruginosa*, *Acinetobacter baumannii* and *Escherichia coli*. Herein we report a detailed mechanistic study using fluorescence labeled analogs bearing fluorescein (**G3KL-Fluo**) or dansyl (**G3KL-Dansyl**), which show a similar bioactivity profile as **G3KL**. Imaging bacterial killing by super-resolution stimulated emission depletion (STED) microscopy, time-lapse imaging and transmission electron microscopy (TEM) reveals that the dendrimer localizes at the bacterial membrane, induces membrane depolarization and permeabilization, and destroys the outer leaflet and the inner membrane. **G3KL** accumulates in bacteria against which it is active, however it only weakly penetrates into eukaryotic cells without inducing significant toxicity. **G3KL** furthermore binds to lipopolysaccharide (LPS) and inhibits LPS induced release of TNF-α by macrophages similarly to polymyxin B. Taken together, these experiments show that **G3KL** behaves as a potent membrane disruptive antimicrobial peptide.

Keywords: bacterial membranes, STED microscopy, Pseudomonas aeruginosa, cell penetrating peptides, polymyxin B

The number of human infections caused by multidrug-resistant bacteria consistently increased since the 1980s. In 2013, multidrug-resistant bacteria *A. baumannii* and *P. aeruginosa* were listed among the top 18 antibiotic resistance threats by the United States CDC (Center for Disease Control and Prevention). In February 2017, both pathogens, together with Enterobacteriaceae were considered as the most critical human pathogens by World Health Organization for which new antibiotics are urgently needed.[1]

One of the approaches to address the challenge of multidrug resistant bacteria consists in designing new analogs of antimicrobial peptides (AMPs), also called host-defense peptides, a broad class of natural products occurring in microorganisms, plants and animals as components of innate immunity, most of which consist of cationic and hydrophobic residues folding into amphiphilic and membrane disruptive α-helices in a membrane environment.[2–8] By exploring synthetic peptides with unusual branched topologies,[9] we discovered that peptide dendrimers composed of lysine and leucine, in particular dendrimer **G3KL**, can exert strong antimicrobial effects against multidrug resistant *P. aeruginosa* and *A. baumannii* including multidrug resistant clinical isolates while showing negligible haemolysis and excellent stability towards serum proteolytic degradation, and thus represent a new opportunity to fight these bacteria (Scheme 1).[10,11] **G3KL** furthermore had a positive impact on burn wound-healing processes by a pro-angiogenic effect,[12] displayed significant inhibitory effects on biofilms,[13] and proved to be amenable to optimization towards in vivo use by a virtual screening guided approach.[14,15]

Although structural studies with **G3KL** and related dendrimers did not provide any evidence of a segregation of hydrophobic and cationic residues towards an amphiphilic structure, we observed that **G3KL** disrupts fluorescein-loaded large unilamellar vesicles consisting of the anionic lipid phosphatidyl glycerol and which mimic bacterial membranes but no effect on vesicles consisting of phosphatidyl choline mimicking the eukaryotic cell

membrane.[16,10] Membrane disruption was also supported by typically fast killing kinetics and by transmission electron microscopy (TEM) images showing disrupted cellular structures.[14,17] LPS deletion mutants of *P. aeruginosa* further revealed that **G3KL** remained active on all variants independent of the LPS composition of the bacterial outer membrane.[10] Inspired by microscopic studies with fluorescence labeled analogs of polymyxin B (PMB, a cyclic antimicrobial peptide),[18] cathelicidins (a family of linear AMPs)[19,20] and antimicrobial peptide polymers,[21] we herein set out to use fluorescence imaging to investigate the mechanism of bacterial killing by antimicrobial peptide dendrimer **G3KL** in more detail.

Results and Discussion

Fluorescent probes G3KL-Fluo and G3KL-Dansyl maintain the activity profile of G3KL

To obtain fluorescence labeled analogs of **G3KL** we extended its sequence by an additional side-chain alloc protected lysine residue as the first core residue.[17] After completion of the SPPS sequence,[22,23] we selectively removed the alloc group and coupled the liberated ε-amino group to 5(6)-carboxyfluorescein, dansyl chloride or rhodamine B. Deprotection of the N-terminal Fmoc groups, side-chain deprotection and cleavage from the solid support followed by RP-HPLC purification yielded dendrimers **G3KL-Fluo**, **G3KL-Dansyl** and **G3KL-Rho** (Table 1, Figure 1). For comparison in experiments with eukaryotic cells we also considered the previously reported cell penetrating dendrimer **D1** in it's fluorescein labeled form, which has a similar sequence but shows no antimicrobial activity.[24]

Table 1. Synthesis and antimicrobial activity of fluorescent **G3KL** analogs and control cell penetrating dendrimer **D1**.[a)]

Cpd.	Sequence[b)]	Yield[c)] mg (%)	MS[d)] calcd/obs.	MW of TFA salt[e)]	*P. aeruginosa* PAO1 MIC (μg/mL)	*E. coli* W3110 MIC (μg/mL)	*A. baumannii* ATCC19606 MIC (μg/mL)
G3KL	$(KL)_8(KKL)_4(KKL)_2KKL$	82.3 (12)	4530.39/ 4531.39	7152.39	4	4-8	8
G3KL-Fluo	$(KL)_8(KKL)_4(KKL)_2KKLK$(Fluo)	46.3 (6)	5017.52/ 5017.54	7754.50	4	2	4
G3KL-Dansyl	$(KL)_8(KKL)_4(KKL)_2KKLK$(Dansyl)	47.5 (6)	4892.52/ 4892.53	7628.52	4	4	8
G3KL-Rho	$(KL)_8(KKL)_4(KKL)_2KKLK$(Rho)	19.7 (2)	5084.69/ 5083.71	7820.69	16	8	8
D1	$(RL)_8(KRL)_4(KKK)_2KGYK$(Fluo)	48 (5.2)	5362.52/5362.52	7938.52	>64	>64	>64

[a]Minimal inhibitory concentration (MIC) values in μg/mL were determined by serial ½ dilution in MH medium. None of the compounds showed any activity (MIC > 64 μg/mL) on *K. pneumoniae*. [b]One letter code is for amino acids. Branching diamino acids are in italics. All peptide dendrimers are carboxamides ($CONH_2$) at the C-terminus. [c]Yields given for RP-HPLC purified product. [d]Mass calcd. for M^+, observed by positive-ion mode ESI as M^+ see SI for details. e) Molecular weight of trifluoroacetate salt, used in all weight measurements for activities.

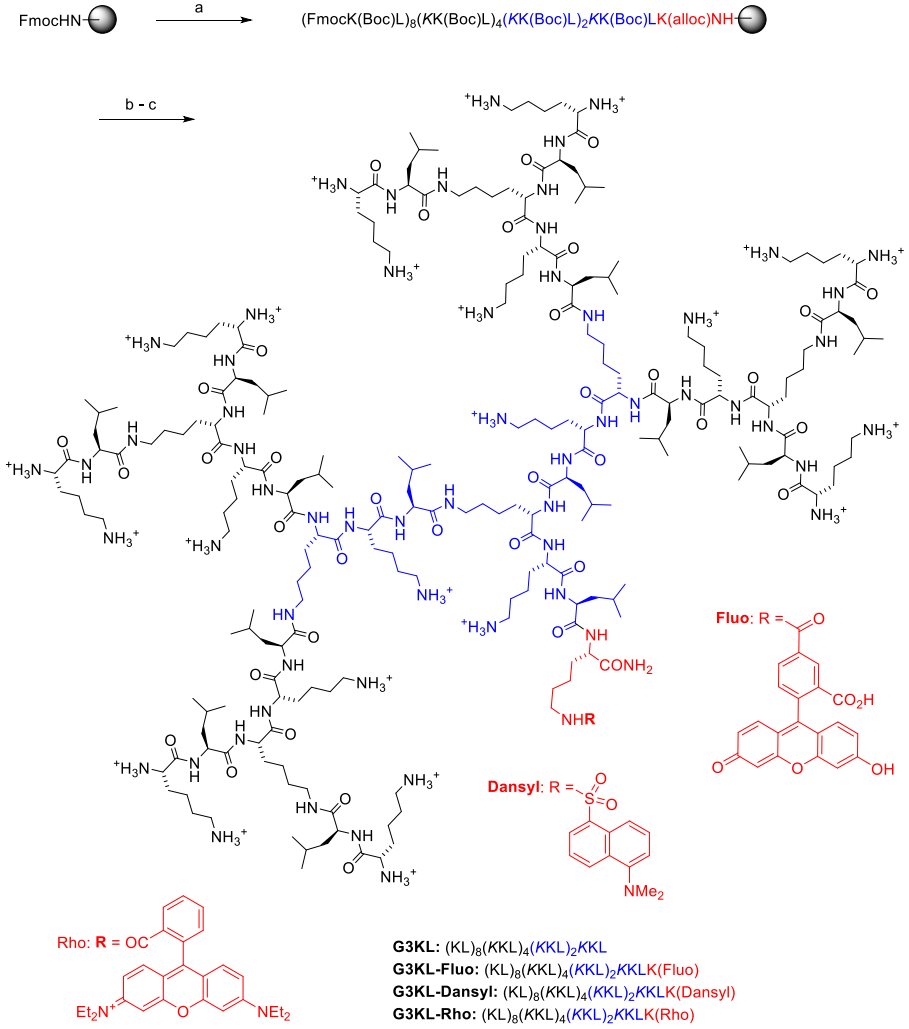

Figure 1. Synthesis of **G3KL** analogs. Conditions: (a) Solid phase peptide synthesis (SPPS): i) 20% v/v piperidine 20 min. 25°C, then wash DMF 3×, MeOH 3× and DCM 3×; ii) FmocAAOH (5 equiv), Oxyma (5 equiv), DIC (7 equiv), NMP, RT, 1.5 h (coupling number and time increased with peptide dendrimer generation). (b) i) Alloc deprotection with $Pd(PPh_3)_4$ (0.25 equiv), $PhSiH_3$ (25 equiv), DCM, 2× 45 min; ii) coupling of the fluorophores to the peptide dendrimer: Dansyl chloride (7 equiv), TEA (7 equiv) in DCM, 5(6)-carboxyfluorescein (7 equiv) and rhodamine B (7 equiv) with Oxyma/DIC in NMP. (c) TFA/TIS/H_2O (95:2.5:2.5), 4h and HPLC purification.

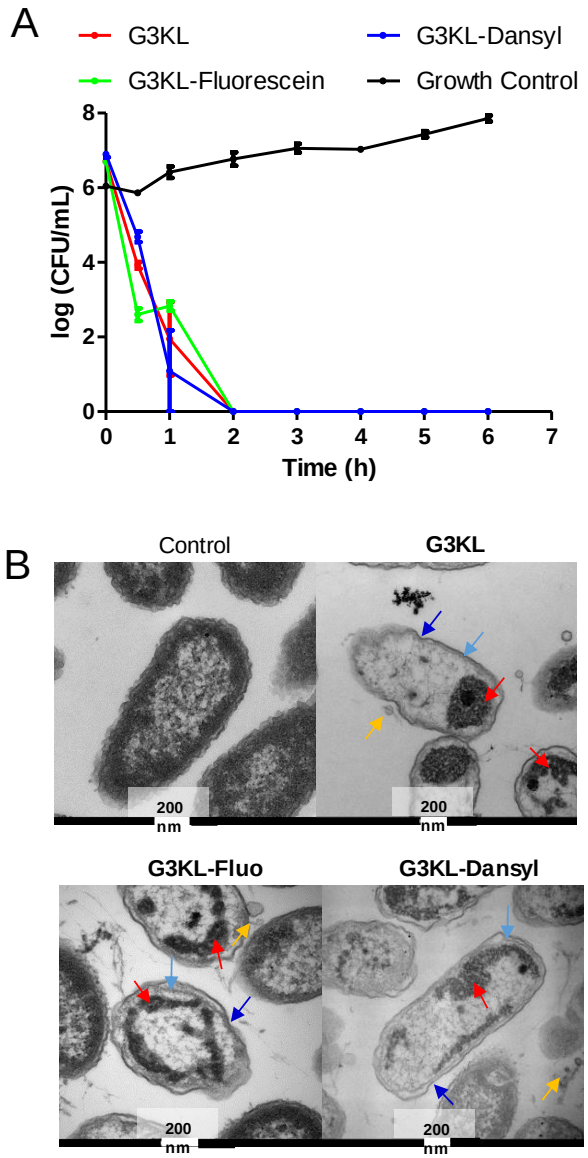

Figure 2. Bacteria killing assay and TEM imaging with **G3KL** and fluorescence labeled analogs. **A.** Static time-kill assay showed a fast decline in *P. aeruginosa* bacterial burden at 37°C in MH medium at 2× MIC for **G3KL** (8 μg/mL), **G3KL-Fluo** (8 μg/mL) and **G3KL-Dansyl** (8 μg/mL). The assay was performed two times in triplicates. **b**. TEM imaging of 10^9 CFU/mL (OD_{600} = 1.0) of *P. aeruginosa* exposed to **G3KL**, **G3KL-Fluo** or **G3KL-Dansyl**. All bacteria were exposed to the same concentration of 40 μg/mL of dendrimer for 60 min in M63 minimal medium. The arrows represent different damages to the bacterial cells. Red: aggregation inside the cell. Blue: bacterial shape change. Light blue: visible broken inner membrane. Enlarged TEM images can be found in the supporting information.

Minimal inhibitory concentration (MIC) profiling showed that **G3KL-Fluo** and **G3KL-Dansyl** had essentially the same activity as **G3KL** against *P. aeruginosa*, *E. coli*, and *A. baumannii*, while **G3KL-Rho** has reduced activity and was therefore not investigated further

(Table 1). Killing kinetics on *P. aeruginosa* at an initial inoculum of ~10^6 cfu/mL showed that **G3KL-Fluo** and **G3KL-Dansyl** behaved similarly to **G3KL**.[14] All three dendrimers induced rapid and significant decline (> 99%) in bacterial burden at 2 × MIC and effectively killed the bacteria after 2 hours (Figure 2A). Furthermore, transmission electron microscopy (TEM) images of *P. aeruginosa* cells exposed to the compounds at 10 × MIC for 1 hour showed that both probes disrupted bacterial cells similarly to unlabeled **G3KL** by causing a change in bacterial shape (or peptidoglycan) (blue arrow), a visible and broken inner membrane (light blue arrow), vesicle-like structures (yellow arrow) and some aggregation inside the cells (red arrow) (Figure 2B).

Super-resolution and confocal microscopy indicate rapid entry of G3KL-Fluo and G3KL-Dansyl into *P. aeruginosa* cells

G3KL-Fluo exhibited a very bright fluorescence suitable for stimulated emission depletion (STED) nanoscopy to track its interaction with bacterial cells. We incubated *P. aeruginosa* cells (10^9 CFU/mL) with **G3KL-Fluo** (10 × MIC, 40 µg/mL) in M63 minimal medium and fixed cells for 2, 5, 15 and 30 minutes. At 2 min. **G3KL-Fluo** was localized at the periphery and inside bacteria. Fluorescence increased at 5 min. with a slightly more intense fluorescence at the bacterial septum of dividing cells, and after 15 minutes bacteria were entirely filled with the compound (Figure 3A). This experiment showed that **G3KL-Fluo** rapidly bound and entered bacterial cells.

In a second imaging experiment by standard confocal imaging, we used **G3KL-Dansyl** in combination with the lipophilic dye **FM4-64** reported to stain the outer[25] or the inner bacterial membrane.[26] The two dyes have different fluorescence excitation and emission wavelength allowing to track the localization of the dendrimer and possible damages to the

cell membrane simultaneously. **FM4-64** indeed stained the bacterial membrane of *P. aeruginosa* cells when incubated alone (both inner and outer membrane were stained). Addition of **G3KL-Dansyl** at 40 µg/mL followed by 15 minutes incubation and fixation resulted in **FM4-64** being dispersed outside and inside the bacteria (Figure 3B). We observed the same effect when first treating with **G3KL-Dansyl** followed by staining with **FM4-64** (Figure S1). We interpret the vesicle-like structures stained by **FM4-64** (yellow arrows) floating outside of the bacteria (green arrows) as the remains of the outer membrane, while the dispersed dye inside bacteria should mark broken inner membrane, in line with the effects of **G3KL-Dansyl** on bacteria observed by TEM (Figure 3B and Figure S2). These membrane disruptive effects are much stronger than those reported when using **FM4-64** to track the effect of PMB on *K. pneumoniae* cells,[18] and of peptide-appended PAMAM dendrimers[21] and multivalent proline peptides on *E. coli* cells.[27]

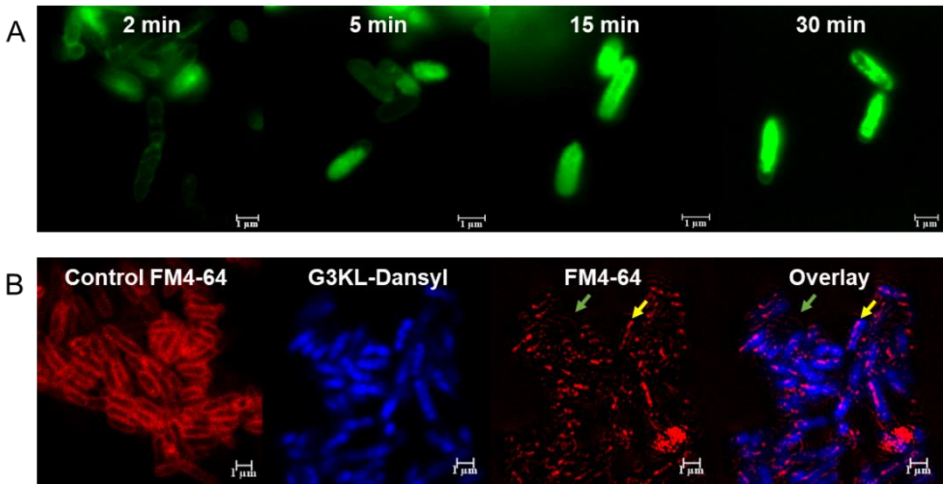

Figure 3. A. Superresolution images of 10^9 CFU/mL (OD_{600} 1.0) of *P. aeruginosa* exposed to 40 µg/mL of **G3KL-Fluo** for 2, 5, 15 and 30 min. Scale bars, 1 µm. The images are representative of two independent experiments. **B.** Confocal microscopy of 10^9 CFU/mL (OD_{600} 1.0) of *P. aeruginosa* incubated with FM4-64 and treated with **G3KL-Dansyl** for 15 min.

Time-lapse imaging shows that G3KL-Fluo enters and permeabilizes *P. aeruginosa* cells

The STED microscopy images above suggested that **G3KL-Fluo** rapidly entered bacterial cells, however images were taken at selected time points with fixed cells. To investigate the

phenomenon closer, we tracked the entry of **G3KL-Fluo** into live *P. aeruginosa* cells in real time by time-lapse confocal imaging similarly to an experiment reported for the AMP cathelicidin cath-2.[20] We performed the experiment in presence of propidium iodide (PI), which becomes fluorescent when binding to DNA and could be used to test whether the dendrimer permeabilized the cells.

To circumvent the swimming capacity of the bacteria in aqueous medium, we trapped the bacteria inside an M63 agarose pad.[20] After adding additional medium to the agarose pad, we adjusted the focus on several bacteria, added PI, initiated the movie, and after 6 min. added our dendrimer. **G3KL-Fluo** immediately started to stain the bacterial surface and within another 5 min. had entirely diffused inside the cells, confirming images obtained by STED microscopy (Figure 4A). Furthermore, we observed that PI, which was initially not visible, also diffused into the cells, however with a delay of approximately 5 min. compared to the dendrimer. This data indicated that the peptide dendrimer diffused or translocated through the membrane into the cytoplasm and triggered permeabilization of bacterial cells, probably through damages at both the outer and inner membrane as observed by TEM (Figure 2B and S2). As a comparison to **G3KL-Fluo**, we also performed time-lapse imaging with unlabeled **G3KL** in the presence of PI. Indeed, PI was rapidly observed within the cells, leading to overexposure of fluorescence within 5 min. after addition of **G3KL**. This experiment showed that labeled and unlabeled dendrimers permeabilized *P. aeruginosa* cells to a similar extent (Figure S3). These permeabilization effects are similar to those reported for the antimicrobial peptide cath-2.[20]

Remarkably, the movie indicated that the fluorescence of **G3KL-Fluo** slightly decreased in the center of the bacteria at 15 min, which might indicate fluorescence quenching due to binding of the dendrimer to DNA (Figure 4A/B).[28,29] Consistent with this hypothesis, incubating **G3KL-Fluo** with plasmid DNA (pEt25*rsl*)[30] induced significant quenching of

fluorescence at N/P = 0.5 and below (excess plasmid, Figure 4C). Quenching reflects a direct binding interaction between the dendrimer and DNA, as evidenced by the decrease in unbound DNA upon addition of unlabeled **G3KL** above N/P = 2.5 as measured the intercalating dye PicoGreen (Figure 4D and S4).[31]

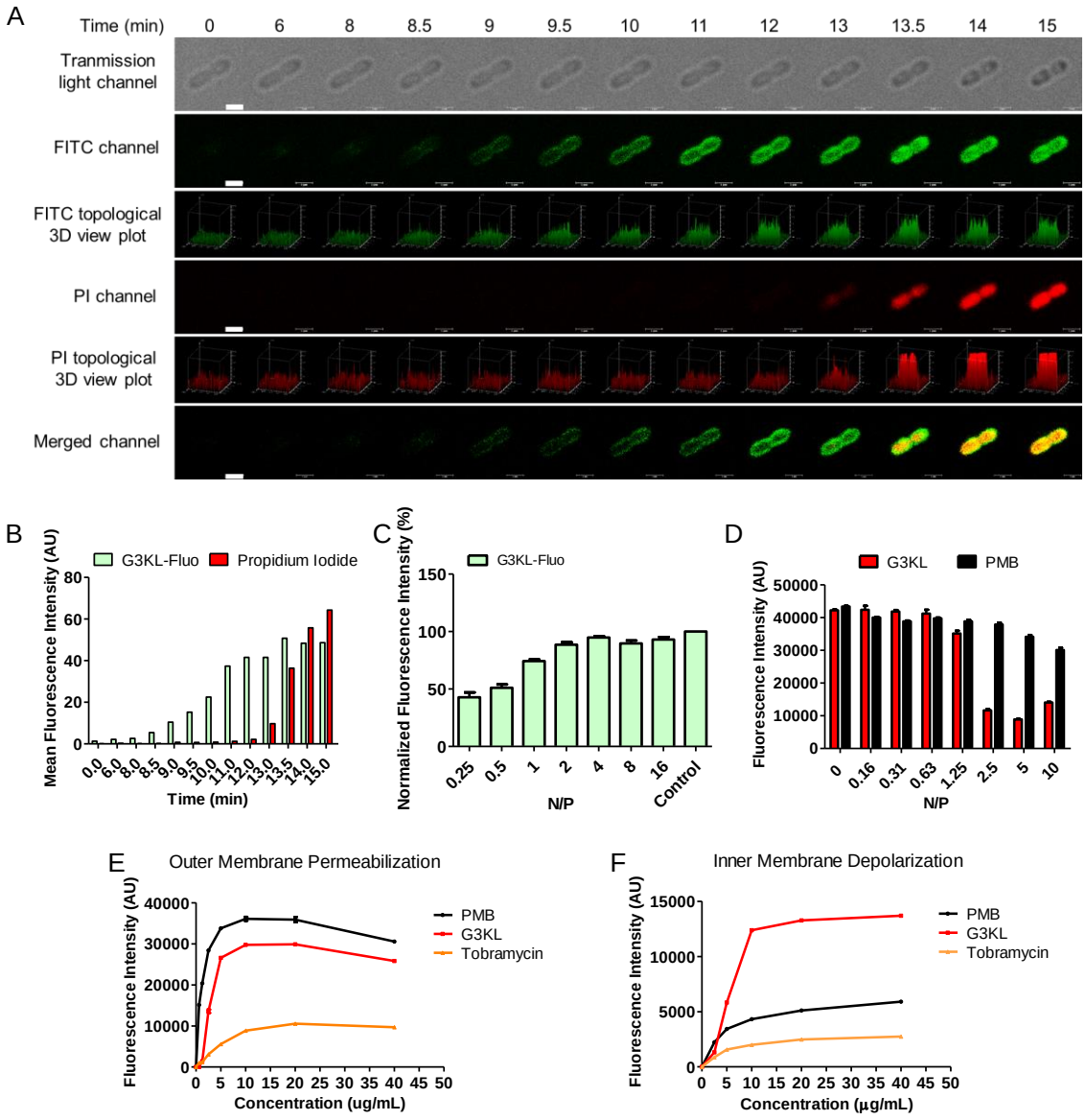

Figure 4. A. Time-lapse imaging of single cell of *P. aeruginosa* exposed to **G3KL-Fluo** at 10x MIC and the nucleic acid selective probe propidium iodide. Scale bar, 1 µm. **B.** Mean fluorescence intensity of **G3KL-Fluo** and PI extracted by using Image J software. **C.** Quenching effect of **G3KL-Fluo** in the presence of the pEt25*rsl* plasmid. **D**. Interaction of **G3KL** and PMB with pEt25*rsl* plasmid by PicoGreen™ assay. **E**. Membrane permeability changes of *P. aeruginosa* induced by PMB, **G3KL** and Tobramycin by NPN assay. **F.** Membrane depolarization of *P. aeruginosa* cells with PMB, **G3KL** and Tobramycin by DiSC3(5) assay. All experiments were performed at least two times in triplicates.

G3KL permeabilizes the outer membrane and depolarizes the inner membrane of *P. aeruginosa* cells.

We performed two additional experiments to measure the effect of our dendrimers on the outer and inner membrane of *P. aeruginosa* cells in comparison to PMB, a membrane active antimicrobial cyclic peptide known to act at the lipopolysaccharide (LPS) in the outer leaflet of the bacterial membrane[32] and tobramycin, an aminoglycoside antibiotic targeting the ribosome that does not affect membrane properties.[33]

In the first experiment, we used the *N*-phenylnaphthylamine (NPN) assay, in which the NPN dye becomes strongly fluorescent in contact with a phospholipid bilayer, indicating permeabilization of the outer membrane[34] PMB was the best permeabilizer exhibiting high fluorescence intensity of NPN at very low concentration of 1.25 µg/mL, reproducing earlier reports in Gram-negative bacteria,[35] while only a very weak signal was observed with tobramycin. While the NPN assay could not be recorded with **G3KL-Fluo** and **G3KL-Dansyl** due to interference with fluorescence excitation and emission wavelengths (Figure S5), the unlabeled dendrimer **G3KL** showed a strong NPN signal at 2.5 µg/mL similarly to PMB, confirming the permeabilization effect on the outer membrane observed in the time-lapse experiment with PI (Figure 4E).

In the second experiment we used the membrane potential-sensitive dye DiSC3(5) to evaluate depolarization of the cytoplasmic (inner) membrane.[36] In this assay **G3KL** exhibited a robust response indicating strong cytoplasmic membrane depolarization at low concentration (Figure 4F**,** Figure S6). In contrast, PMB and tobramycin only showed a weak effect, indicating that these antibiotics do not affect the inner membrane of *P. aeruginosa*. In the case of PMB the absence of inner membrane depolarization is consistent with the fact that the primary interaction site of PMB is Lipid A located at the outer membrane.[32]

G3KL-Fluo and G3KL accumulate in bacteria

Since the microscopy studies above showed that **G3KL-Fluo** bound and internalized into bacteria, we were curious to estimate the amount of dendrimer taken up by the cells. We quantified cellular uptake as the difference between total **G3KL-Fluo** added and unabsorbed dendrimer measured by the fluorescence remaining in the supernatant after high speed centrifugation of the bacteria. For *P. aeruginosa* cells at OD_{600} 1.0 in M63 medium, we found that at an initial concentration of 40 µg/mL **G3KL-Fluo** 80% of the dendrimer was absorbed after 5 min. After 15 min incubation, fluorescence in the supernatant was close to background, indicating complete uptake by the bacteria (Figure 5A). Repeating the experiment with higher starting concentration of **G3KL-Fluo** showed that the maximal uptake corresponded to 32-64 µg/mL **G3KL-Fluo** in the supernatant (Figure S8).

Under the same conditions, uptake was also quantitative with *A. baumannii* and at 60% with *E. coli*, both of which are sensitive to **G3KL-Fluo**, while no significant uptake was observed for methicillin-resistant *Staphylococcus aureus* and *Klebsiella pneumoniae*, against which **G3KL-Fluo** was inactive (Figure 5B). Uptake of the dendrimer was confirmed by confocal microscopy of *A. baumannii* and *E. coli* treated with 40 µg/mL of **G3KL-Fluo**, which showed that the dendrimer not only binds to the cell surface but also penetrates the cells as in the case of *P. aeruginosa* discussed above (Figure 3 and S7). These experiments showed that **G3KL-Fluo** only accumulated in bacteria against which it was active. The absence of uptake by *S. aureus* probably reflects the very different composition of the bacterial cell envelope of Gram-positive versus Gram-negative bacteria,[37] while in the case of *K. pneumoniae* uptake of **G3KL**-Fluo might be blocked by the polysaccharide capsule.[38]

To compare whether labeled and unlabeled compounds were absorbed in the same range, we treated the bacteria (10^9 CFU/mL) with **G3KL**, **G3KL-Fluo** and PMB at various

concentrations (32, 64 and 128 µg/mL) in M63 minimal medium. After 60 minutes, we centrifuged the bacteria at maximal speed, isolated the supernatant and used it as the starting concentration for MIC determination to determine the remaining antibacterial activity and therefore the amount of compound left in the supernatant in comparison with a reference untreated sample in the same medium. Note that while the activity of PMB decreased from 0.25 µg/mL in MH to 4 µg/mL in M63 due the presence of magnesium in the latter medium,[39] the activity of **G3KL** and **G3KL-Fluo** was the same (4 µg/mL) in both media (Table S1).

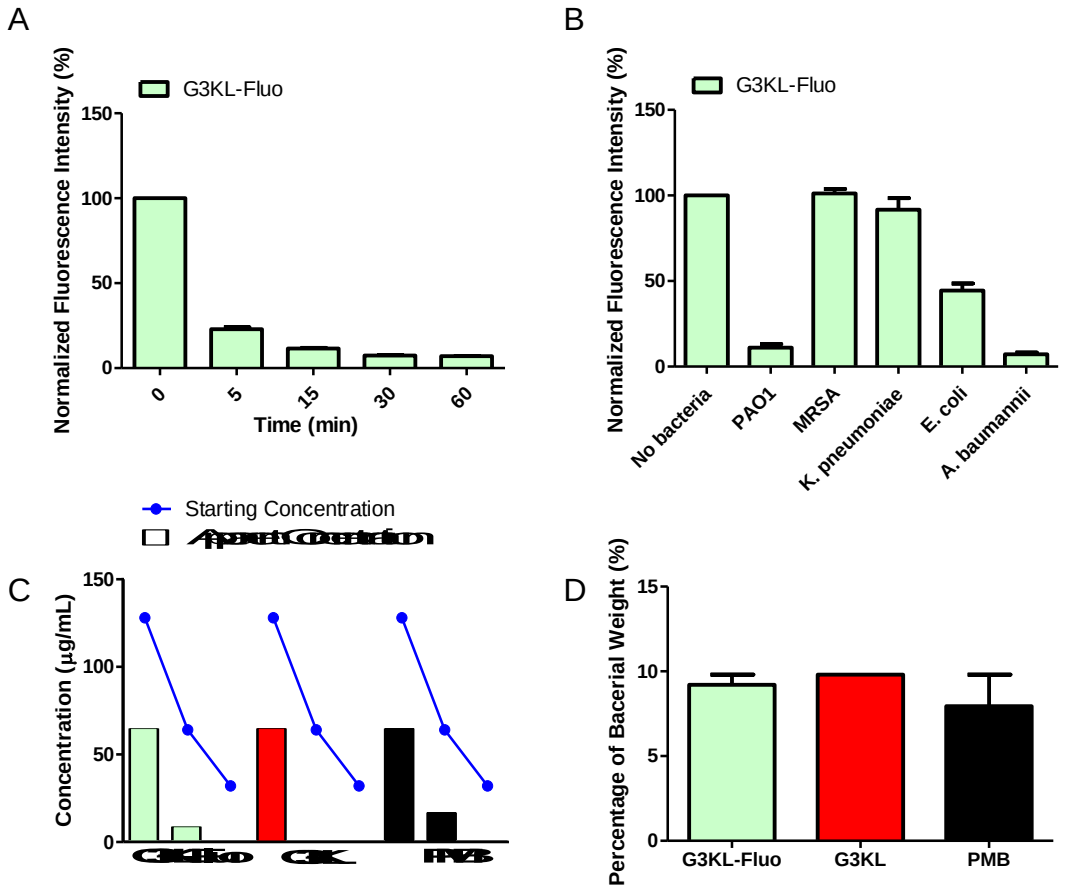

Figure 5. Quantification of **G3KL-Fluo** taken up by 10^9 CFU/mL (OD_{600} 1.0) of *P. aeruginosa* cells. **A**. Fluorescence measurement of the supernatant from the treated samples at 40 µg/mL. **B.** Measurement of the excess fluorescence in the supernatant after exposing the bacteria *P. aeruginosa*, MRSA, *K. pneumoniae*, *E. coli* and *A. baumannii* to **G3KL-Fluo** at 40 µg/mL in M63 medium for 60 min. **C.** Starting and Apparent Concentration of **G3KL**, **G3KL-Fluo** and PMB in *P. aeruginosa* PAO1 after 60 min at 37 °C. **D.** Total amount of **G3KL**, **G3KL-Fluo** and PMB in 1 g of bacteria. All experiments were performed two times in triplicates.

The results showed that labeled and unlabeled peptide dendrimers were taken up in comparable amounts by *P. aeruginosa* cells (Figure 5C). The amounts of 64 μg/mL **G3KL-Fluo** and 56-64 μg/mL **G3KL** for 10^9 CFU/mL determined by the MIC method precisely matched the uptake measured by fluorescence with **G3KL-Fluo** (Figure S8). Bacterial uptake of PMB (40-64 μg/mL) by *P. aeruginosa* was comparable to that of our dendrimers and matched the data reported for the uptake of antimicrobial peptide PMAP-23 by high density *E. coli*.[40] Considering the dimensions of *P. aeruginosa* cells estimated by TEM to determine bacterial volume (Figure S2) and assuming a density of 1 g/mL for the bacterial cell, these data implied that these antibacterial compounds accumulate in *P. aeruginosa* up to 5-10% of bacterial weight, corresponding to at least a 100-fold concentration from the medium (Figure 5D).

G3KL-Fluo and G3KL penetrate but are non-toxic and do not accumulate in mammalian cells

To test if **G3KL-Fluo** had cell penetrating properties in mammalian cells, we measured cellular uptake in HeLa and CHO cells by imaging flow cytometry (ImageStream) in comparison to **D1**, a peptide dendrimer optimized for cellular uptake,[24] and the cell penetrating linear peptides **TAT** and $\mathbf{R_9}$ (nona-arginine), all of which were labeled with fluorescein.[41,42] Analysis of cellular uptake by flow cytometry showed that **G3KL-Fluo** entered cells to the same level as **TAT**, corresponding to 10% uptake in HeLa and 30% in CHO cells compared to **D1** and 20% compared to $\mathbf{R_9}$ peptide in both cell lines (Figure 6A, Figure S10). Quantifying uptake by the difference method used above with bacteria showed that the amount of compound actually taken up by the cells was not significant with any of the four compounds tested (Figure 6B). We also found that **G3KL-Fluo** and **G3KL** were not toxic to both cell lines, with IC_{50} values well above their MIC values against bacteria (IC_{50} =

135 µM; ~1,000 µg/mL, Figure 6C/D). On the other hand, **G3KL-Dansyl** showed significant toxicity (IC_{50} = 15 µM; ~107 µg/mL) in both cell lines, showing that minor structural changes may affect activity even in the relatively large peptide dendrimer molecule.

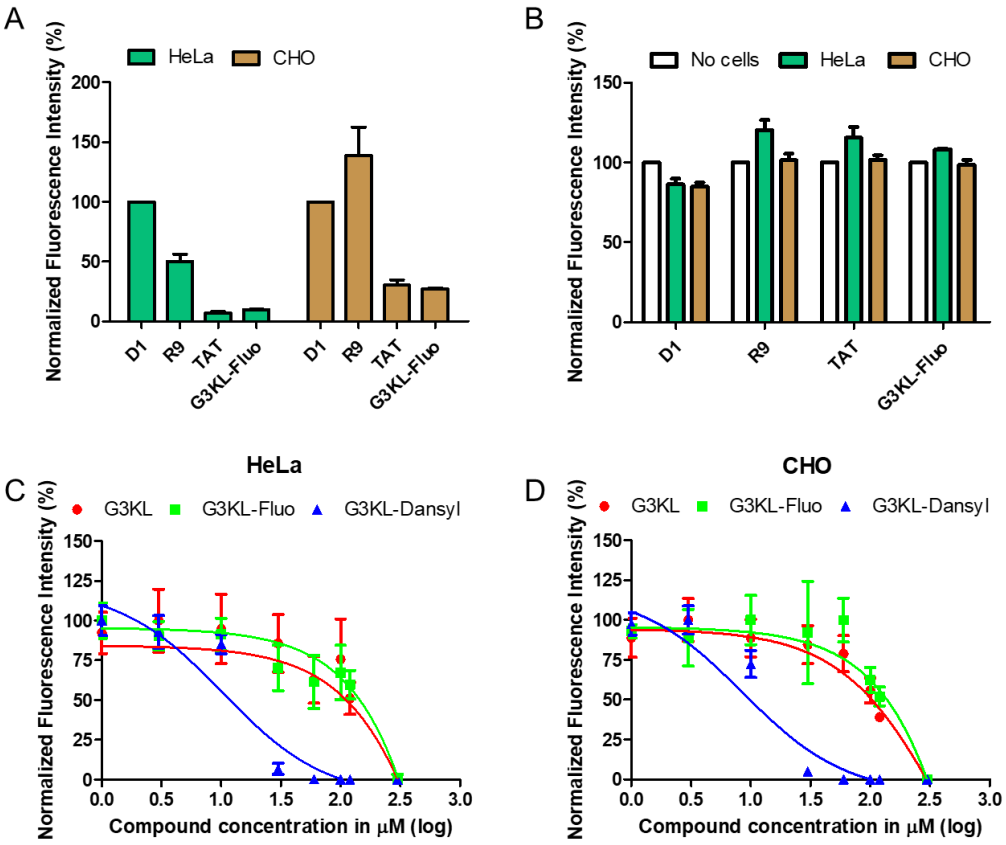

Figure 6. A. Quantification of cell penetrating peptide and peptide dendrimers in HeLa and CHO cells at 10 µM for 60 minutes in the presence of DMEM containing 1% BSA at 37°C and 5% CO_2 by imaging flow cytometry. **B.** Measurement of the excess of fluorescence in the supernatant after exposing HeLa and CHO cells to the cell penetrating peptide and peptide dendrimers at 10 µM for 60 minutes. Cytotoxicity of **G3KL**, **G3KL-Fluo** and **G3KL-Dansyl** in HeLa (**C**) and CHO (**D**) cells in DMEM containing 10% FBS. All experiments were performed two times in triplicates.

G3KL binds and inactivates Endotoxin lipopolysaccharide (LPS), and vice versa

Most cationic AMPs including PMB and the cathelicidin family of AMPs bind to the endotoxin lipopolysaccharide (LPS), which is the major component of the outer membrane of Gram-negative bacteria,[43] and thereby have the beneficial effect to inhibit the release of pro-inflammatory cytokines such as TNF-α from macrophages induced by binding of LPS to toll-

like receptor TLR4,[44,45] and thereby to attenuate septic shock.[46–48] We obtained a first evidence of a binding interaction between our dendrimers and LPS by a quenching effect of LPS on **G3KL-Fluo** probably caused by autoquenching due to concentration upon binding to LPS aggregates (Figure 7A).[49] Evidence for unlabeled **G3KL** binding to LPS was next obtained by tracking LPS induced expression of intracellular TNF-α in mouse macrophages RAW264.7 by Western blot (WB, Figure 7B). Indeed, **G3KL** (10 µM, 72 µg/mL) blocked TNF-α expression induced by LPS (0.1 µg/mL) when the experiment was performed in DMEM containing 1% FBS, similarly to the effect observed by PMB (10 µM, 14 µg/mL) (Figure 7B). When the experiment was performed in the presence of 10% FBS by contrast we only observed TNF-α inhibition by PMB as previously reported,[50,51] while **G3KL** was inactive, suggesting a weaker and less selective binding to LPS versus serum proteins compared to PMB (Figure 7C).

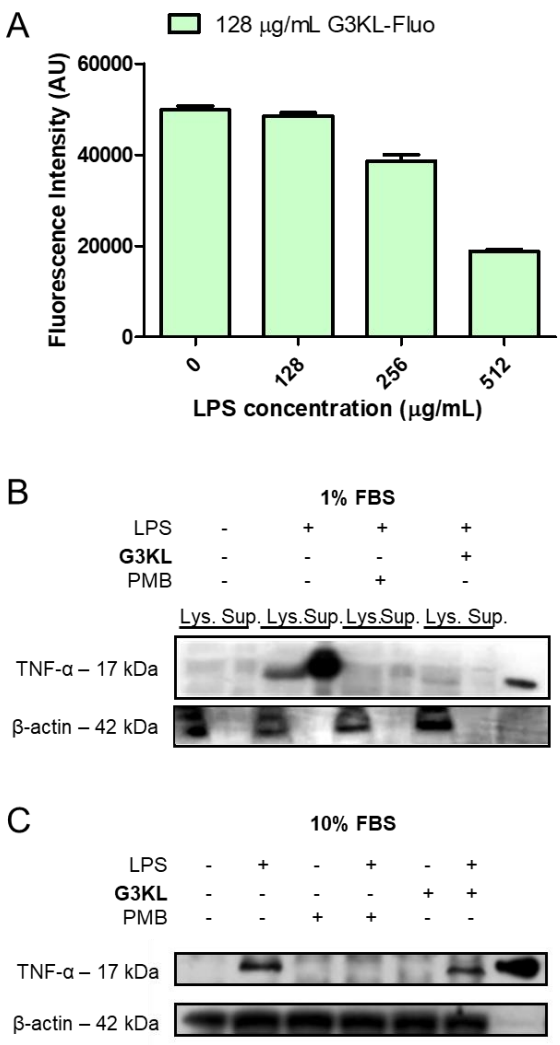

Figure 7. Fluorescence measurement of **G3KL-Fluo** at 128 µg/mL mixed with increasing concentrations of LPS. The experiment was performed two times in triplicates. (**A**). Effect of antimicrobial peptide dendrimer **G3KL** and PMB on the expression of inflammatory cytokine TNF-α by Western blot. Total proteins were run on 12% Bolt Tris Glycine Plus gels in reducing condition (dithiothreitol at 95°C for 5 min). Separated proteins were immunoblotted with anti-TNF-α antibody. The immunoreactive bands of TNF-α in RAW264.7 cells treated with or without LPS ± the compounds (PMB 14 µg/mL, 10 µM or **G3KL**, 72 µg/mL 10 µM) for a total time of 3 hours in DMEM containing 1% FBS (**B**) or 10% FBS (**C**). (**B**) and (**C**) were performed two times.

Besides its effect on TNF-α release, the binding interaction between LPS and antimicrobial compounds should also result in decreased antimicrobial activity. To test this hypothesis, we measured the antibacterial activity of **G3KL**, PMB and tobramycin on *E. coli*, *P. aeruginosa* and *A. baumannii* in the presence of LPS. The presence of a small amount of LPS in the medium (5 µg/mL) indeed reduced the antibacterial activity PMB but not of **G3KL** or tobramycin (Table 2, left part). On the other hand, further increasing LPS in the presence of a

constant amount **G3KL** (8 µg/mL) eventually also blocked its activity in all three strains tested ([LPS] ≥ 32-64 µg/mL), while tobramycin remained unaffected (Table 2, right part).

The data indicated that a 4-fold excess by weight of LPS was necessary to block the activity of **G3KL**, which is comparable to PMB at 0.5 µg/mL losing its activity with 2-4 µg/mL of LPS. In the case of PMB which carries five positive charges for MW = 1203.5 kDa, this stoichiometry corresponds to charge neutralization assuming MW = 10 kDa for LPS and that the serotype used (O111) contains 6-10 negative charges.[52] The same applies to **G3KL** when considering acid-base titration indicating that at physiological pH the amino termini are present as free base (NH_2), while all lysine side chains are protonated (NH_3^+), which overall corresponds to 15 positive charges for **G3KL** at pH 7.4 for a MW of 4534.30 kDa (Table 3, Figure S11).

Table 2. Minimum concentration of LPS required to block the activity of PMB and **G3KL** in *E. coli* W3110 and *P. aeruginosa* PAO1 and *A. baumannii* (ATCC19606).

	PMB[a] (-/+ 5 µg/mL LPS)	**G3KL**[a] (-/+ 5 µg/mL LPS)	Tobra[a] (-/+ 5 µg/mL LPS)	LPS[b] (+ 0.5 µg/mL PMB)	LPS[b] (+ 8 µg/mL **G3KL**)	LPS[b] (+ 4 or 8 µg/mL Tobra)
E. coli	0.125 / 0.5	4-8 / 8	0.25 / 0.25	2-4*	32-64*	> 64*
P. aeruginosa	0.25 / 2	4 / 4	0.25 / 0.25	1-2*	64*	> 64*
A. baumannii	0.25 / 2	8 / 8	2 / 2	4-8*	32-64*	> 64*

a) The minimum inhibitory concentration in µg/mL was determined in MH medium. b) The minimum concentration of LPS in µg/mL was determined in MH medium containing Polymyxin, **G3KL** or Tobramycin. * Amount of LPS necessary to inhibit the activity of PMB, **G3KL**, Tobra at 2 × MIC. The experiments were performed at least two times in triplicates.

Table 3. Ratio of molecular charges between **G3KL**, PMB and LPS.

	MW[a]	Number of charges	MW/charges	Ratio LPS/compound charge
G3KL	4534	15	302.3	3.3 – 5.5
PMB	1204	5	241	4.1 – 6.9
LPS	10000	6 – 10[b]	1000 - 1666	-

[a] MW without counter ions in g/mol [b] data from reference[52]

We believe that inactivation by LPS binding might explain the regrowth of *P. aeruginosa* after treatment with PMB often observed in time-kill experiments[53] since PMB is usually applied in low amounts (0.5 μg/mL). By contrast, the absence of any regrowth in time kill experiments with our dendrimers is probably explained by the much higher amounts applied (8 μg/mL) which provide excess of antibacterial compound compared to the amount of LPS that can be released by bacteria.

Conclusion

The fluorescence imaging and mechanistic studies with fluorescence labeled analogs of antimicrobial peptide dendrimer **G3KL** presented above reveal its bacterial killing mechanism and show that **G3KL** behaves as a membrane disruptive AMP against Gram-negative bacteria. When compared with other AMPs, **G3KL** disrupts bacterial membranes to a larger extent than PMB as observed by TEM[14,17] and by confocal microscopy (Figure 3), but produces the same overall cell permeabilization effects as cathelicidin cath-2 by time-lapse imaging of propidium iodide uptake (Figure 4A-D).[20] **G3KL** furthermore induces a similar level of outer membrane permeabilization as cathelicidin PMAP-36[54] and PMB by the NPN assay (Figure 4E) and in addition depolarizes the inner membrane to the same extent as Gramicidin S (Figure 4F).[35] The cell-penetrating properties of **G3KL** (Figure 6) and its LPS neutralizing abilities (Figure 7, Table 2-3) are further attributes of typical membrane disruptive AMPs.

Most strikingly, **G3KL** accumulates in *P. aeruginosa*, *A. baumannii* and *E. coli* cells, against which it is active, but does not accumulate in *K. pneumoniae* or MRSA, against which it is inactive (Figure 5). Our observation of accumulation of our dendrimer **G3KL** and PMB in bacteria, which has also been noted for cathelicidin PMAP-23,[40] is probably a general feature of membrane disruptive AMPs. We also believe that our observations with **G3KL** are

representative of the mechanism of action of recently reported antimicrobial peptide dendrimer analogs of **G3KL**.[14,15,17]

Methods

Procedures for peptide synthesis, microbiology, cell culture, microscopy, and analytical data for all peptides, are described in the supporting information.

Associated Content

Supporting Information. The supporting information is available free of charge on the ACS Publication website.

Synthesis and characterization of all peptides, microbiology, microscopy.

Author Information

Corresponding Author. *E-mail: jean-louis.reymond@dcb.unibe.ch.

Author Contributions. BHG designed and performed the entire study, interpreted data and wrote the paper. TNS performed antimicrobial activity assays. SJ designed and supervised microscopy experiments, interpreted data, and wrote the paper. TD and JLR designed and supervised the study, interpreted data and wrote the paper.

Notes. The authors declare no competing financial interest.

Acknowledgments

This work was supported financially by the Swiss National Science Foundation (Grant no. 200020_178998, 407240_167048, IZLCZ2_155982).

References

(1) World Health Organization. (2017) WHO Priority Pathogens List for R&D of New Antibiotics.

(2) Zasloff, M. (2002) Antimicrobial Peptides of Multicellular Organisms. *Nature 415*, 389–395. https://doi.org/10.1038/415389a.

(3) Nguyen, L. T.; Haney, E. F.; Vogel, H. J. (2011) The Expanding Scope of Antimicrobial Peptide Structures and Their Modes of Action. *Trends Biotechnol. 29*, 464–472. https://doi.org/10.1016/j.tibtech.2011.05.001.

(4) Mojsoska, B.; Jenssen, H. (2015) Peptides and Peptidomimetics for Antimicrobial Drug Design. *Pharmaceuticals 8*, 366–415. https://doi.org/10.3390/ph8030366.

(5) Czaplewski, L.; Bax, R.; Clokie, M.; Dawson, M.; Fairhead, H.; Fischetti, V. A.; Foster, S.; Gilmore, B. F.; Hancock, R. E.; Harper, D.; Henderson, I. R.; Hilpert, K.; Jones, B. V.; Kadioglu, A.; Knowles, D.; Olafsdottir, S.; Payne, D.; Projan, S.; Shaunak, S.; Silverman, J.; Thomas, C. M.; Trust, T. J.; Warn, P.; Rex, J. H. (2016) Alternatives to Antibiotics-a Pipeline Portfolio Review. *Lancet Infect. Dis. 16*, 239–251. https://doi.org/10.1016/s1473-3099(15)00466-1.

(6) Acedo, J. Z.; Chiorean, S.; Vederas, J. C.; van Belkum, M. J. (2018) The Expanding Structural Variety among Bacteriocins from Gram-Positive Bacteria. *FEMS Microbiol. Rev. 42*, 805–828. https://doi.org/10.1093/femsre/fuy033.

(7) Amso, Z.; Hayouka, Z. (2019) Antimicrobial Random Peptide Cocktails: A New Approach to Fight Pathogenic Bacteria. *Chem. Commun. 55*, 2007–2014. https://doi.org/10.1039/c8cc09961h.

(8) Torres, M. D. T.; Sothiselvam, S.; Lu, T. K.; de la Fuente-Nunez, C. (2019) Peptide Design Principles for Antimicrobial Applications. *J. Mol. Biol.* https://doi.org/10.1016/j.jmb.2018.12.015.

(9) Reymond, J. L.; Darbre, T. (2013) Expanding the Topological Space of Bioactive Peptides. *Chimia 67*, 864–867. https://doi.org/10.2533/chimia.2013.864.

(10) Stach, M.; Siriwardena, T. N.; Kohler, T.; van Delden, C.; Darbre, T.; Reymond, J. L. (2014) Combining Topology and Sequence Design for the Discovery of Potent Antimicrobial Peptide Dendrimers against Multidrug-Resistant Pseudomonas Aeruginosa. *Angew. Chem., Int. Ed. Engl. 53*, 12827–12831. https://doi.org/10.1002/anie.201409270.

(11) Pires, J.; Siriwardena, T. N.; Stach, M.; Tinguely, R.; Kasraian, S.; Luzzaro, F.; Leib, S. L.; Darbre, T.; Reymond, J. L.; Endimiani, A. (2015) In Vitro Activity of the Novel Antimicrobial Peptide Dendrimer G3KL against Multidrug-Resistant Acinetobacter Baumannii and Pseudomonas Aeruginosa. *Antimicrob. Agents Chemother. 59*, 7915–7918. https://doi.org/10.1128/aac.01853-15.

(12) Abdel-Sayed, P.; Kaeppeli, A.; Siriwardena, T.; Darbre, T.; Perron, K.; Jafari, P.; Reymond, J. L.; Pioletti, D. P.; Applegate, L. A. (2016) Anti-Microbial Dendrimers against Multidrug-Resistant P. Aeruginosa Enhance the Angiogenic Effect of Biological Burn-Wound Bandages. *Sci. Rep. 6*, 1–10. https://doi.org/10.1038/srep22020.

(13) Han, X.; Liu, Y.; Ma, Y.; Zhang, M.; He, Z.; Siriwardena, T. N.; Xu, H.; Bai, Y.; Zhang, X.; Reymond, J.-L.; Qiao, M. (2019) Peptide Dendrimers G3KL and TNS18

Inhibit Pseudomonas Aeruginosa Biofilms. *Appl. Microbiol. Biotechnol. 103*, 5821–5830. https://doi.org/10.1007/s00253-019-09801-3.

(14) Siriwardena, T. N.; Capecchi, A.; Gan, B. H.; Jin, X.; He, R.; Wei, D.; Ma, L.; Kohler, T.; van Delden, C.; Javor, S.; Reymond, J. L. (2018) Optimizing Antimicrobial Peptide Dendrimers in Chemical Space. *Angew. Chem., Int. Ed. Engl. 57*, 8483–8487. https://doi.org/10.1002/anie.201802837.

(15) Siriwardena, T. N.; Lüscher, A.; Köhler, T.; van Delden, C.; Javor, S.; Reymond, J.-L. (2019) Antimicrobial Peptide Dendrimer Chimera. *Helv. Chim. Acta 102*, e1900034. https://doi.org/10.1002/hlca.201900034.

(16) Hennig, A.; Gabriel, G. J.; Tew, G. N.; Matile, S. (2008) Stimuli-Responsive Polyguanidino-Oxanorbornene Membrane Transporters as Multicomponent Sensors in Complex Matrices. *J. Am. Chem. Soc. 130*, 10338–10344. https://doi.org/10.1021/ja802587j.

(17) Siriwardena, T. N.; Stach, M.; He, R.; Gan, B.-H.; Javor, S.; Heitz, M.; Ma, L.; Cai, X.; Chen, P.; Wei, D.; Li, H.; Ma, J.; Köhler, T.; van Delden, C.; Darbre, T.; Reymond, J.-L. (2018) Lipidated Peptide Dendrimers Killing Multidrug-Resistant Bacteria. *J. Am. Chem. Soc. 140*, 423–432. https://doi.org/10.1021/jacs.7b11037.

(18) Deris, Z. Z.; Swarbrick, J. D.; Roberts, K. D.; Azad, M. A. K.; Akter, J.; Horne, Andrew. S.; Nation, R. L.; Rogers, K. L.; Thompson, P. E.; Velkov, T.; Li, J. (2014) Probing the Penetration of Antimicrobial Polymyxin Lipopeptides into Gram-Negative Bacteria. *Bioconj. Chem. 25*, 750–760. https://doi.org/10.1021/bc500094d.

(19) Sochacki, K. A.; Barns, K. J.; Bucki, R.; Weisshaar, J. C. (2011) Real-Time Attack on Single Escherichia Coli Cells by the Human Antimicrobial Peptide LL-37. *Proc. Natl. Acad. Sci. U. S. A. 108*, E77–E81. https://doi.org/10.1073/pnas.1101130108.

(20) Schneider, V. A. F.; Coorens, M.; Ordonez, S. R.; Tjeerdsma-van Bokhoven, J. L. M.; Posthuma, G.; van Dijk, A.; Haagsman, H. P.; Veldhuizen, E. J. A. (2016) Imaging the Antimicrobial Mechanism(s) of Cathelicidin-2. *Sci. Rep. 6*, 32948. https://doi.org/10.1038/srep32948.

(21) Lam, S. J.; O'Brien-Simpson, N. M.; Pantarat, N.; Sulistio, A.; Wong, E. H. H.; Chen, Y.-Y.; Lenzo, J. C.; Holden, J. A.; Blencowe, A.; Reynolds, E. C.; Qiao, G. G. (2016) Combating Multidrug-Resistant Gram-Negative Bacteria with Structurally Nanoengineered Antimicrobial Peptide Polymers. *Nat. Microbiol. 1*, 16162. https://doi.org/10.1038/nmicrobiol.2016.162.

(22) Amblard, M.; Fehrentz, J.-A.; Martinez, J.; Subra, G. (2006) Methods and Protocols of Modern Solid Phase Peptide Synthesis. *Mol. Biotechnol. 33*, 239–254. https://doi.org/10.1385/MB:33:3:239.

(23) Reymond, J.-L.; Darbre, T. (2012) Peptide and Glycopeptide Dendrimer Apple Trees as Enzyme Models and for Biomedical Applications. *Org. Biomol. Chem. 10*, 1483–1492. https://doi.org/10.1039/c2ob06938e.

(24) Eggimann, G. A.; Blattes, E.; Buschor, S.; Biswas, R.; Kammer, S. M.; Darbre, T.; Reymond, J. L. (2014) Designed Cell Penetrating Peptide Dendrimers Efficiently Internalize Cargo into Cells. *Chem. Commun. 50*, 7254–7257. https://doi.org/10.1039/c4cc02780a.

(25) Pilizota, T.; Shaevitz, J. W. (2012) Fast, Multiphase Volume Adaptation to Hyperosmotic Shock by Escherichia Coli. *PLOS ONE 7*, e35205. https://doi.org/10.1371/journal.pone.0035205.

(26) Fishov, I.; Woldringh, C. L. (1999) Visualization of Membrane Domains in Escherichia Coli. *Mol. Microbiol. 32*, 1166–1172. https://doi.org/10.1046/j.1365-2958.1999.01425.x.

(27) Li, W.; O'Brien-Simpson, N. M.; Tailhades, J.; Pantarat, N.; Dawson, R. M.; Otvos, L.; Reynolds, E. C.; Separovic, F.; Hossain, M. A.; Wade, J. D. (2015) Multimerization of a Proline-Rich Antimicrobial Peptide, Chex-Arg20, Alters Its Mechanism of Interaction with the Escherichia Coli Membrane. *Chem. Biol. 22*, 1250–1258. https://doi.org/10.1016/j.chembiol.2015.08.011.

(28) Tworzydło, M.; Polit, A.; Mikołajczak, J.; Wasylewski, Z. (2005) Fluorescence Quenching and Kinetic Studies of Conformational Changes Induced by DNA and CAMP Binding to CAMP Receptor Protein from Escherichia Coli. *FEBS J. 272*, 1103–1116. https://doi.org/10.1111/j.1742-4658.2005.04540.x.

(29) Kozlov, A. G.; Galletto, R.; Lohman, T. M. (2012) SSB–DNA Binding Monitored by Fluorescence Intensity and Anisotropy. *Methods Mol. Biol. 922*, 55–83. https://doi.org/10.1007/978-1-62703-032-8_4.

(30) Kostlánová, N.; Mitchell, E. P.; Lortat-Jacob, H.; Oscarson, S.; Lahmann, M.; Gilboa-Garber, N.; Chambat, G.; Wimmerová, M.; Imberty, A. (2005) The Fucose-Binding Lectin from Ralstonia Solanacearum. A New Type of β-Propeller Architecture Formed by Oligomerization and Interacting with Fucoside, Fucosyllactose, and Plant

Xyloglucan. *J. Biol. Chem. 280*, 27839–27849. https://doi.org/10.1074/jbc.M505184200.

(31) Dragan, A. I.; Casas-Finet, J. R.; Bishop, E. S.; Strouse, R. J.; Schenerman, M. A.; Geddes, C. D. (2010) Characterization of PicoGreen Interaction with DsDNA and the Origin of Its Fluorescence Enhancement upon Binding. *Biophys. J. 99*, 3010–3019. https://doi.org/10.1016/j.bpj.2010.09.012.

(32) Velkov, T.; Thompson, P. E.; Nation, R. L.; Li, J. (2010) Structure--Activity Relationships of Polymyxin Antibiotics. *J. Med. Chem. 53*, 1898–1916. https://doi.org/10.1021/jm900999h.

(33) Yang, G.; Trylska, J.; Tor, Y.; McCammon, J. A. (2006) Binding of Aminoglycosidic Antibiotics to the Oligonucleotide A-Site Model and 30S Ribosomal Subunit: Poisson−Boltzmann Model, Thermal Denaturation, and Fluorescence Studies. *J. Med. Chem. 49*, 5478–5490. https://doi.org/10.1021/jm060288o.

(34) Helander, I. M.; Mattila-Sandholm, T. (2000) Fluorometric Assessment of Gram-Negative Bacterial Permeabilization. *J. Appl. Microbiol. 88*, 213–219. https://doi.org/10.1046/j.1365-2672.2000.00971.x.

(35) Zhang, L.; Dhillon, P.; Yan, H.; Farmer, S.; Hancock, R. E. W. (2000) Interactions of Bacterial Cationic Peptide Antibiotics with Outer and Cytoplasmic Membranes of Pseudomonas Aeruginosa. *Antimicrob. Agents Chemother. 44*, 3317–3321.

(36) Te Winkel, J. D.; Gray, D. A.; Seistrup, K. H.; Hamoen, L. W.; Strahl, H. (2016) Analysis of Antimicrobial-Triggered Membrane Depolarization Using Voltage Sensitive Dyes. *Front. Cell Dev. Biol. 4*. https://doi.org/10.3389/fcell.2016.00029.

(37) Malanovic, N.; Lohner, K. (2016) Gram-Positive Bacterial Cell Envelopes: The Impact on the Activity of Antimicrobial Peptides. *Biochim. Biophys. Acta 1858*, 936–946. https://doi.org/10.1016/j.bbamem.2015.11.004.

(38) Campos, M. A.; Vargas, M. A.; Regueiro, V.; Llompart, C. M.; Albertí, S.; Bengoechea, J. A. (2004) Capsule Polysaccharide Mediates Bacterial Resistance to Antimicrobial Peptides. *Infect. Immun. 72*, 7107–7114. https://doi.org/10.1128/IAI.72.12.7107-7114.2004.

(39) Chen, C.-C. H.; Feingold, D. S. (1972) Locus of Divalent Cation Inhibition of the Bactericidal Action of Polymyxin B. *Antimicrob. Agents Chemother. 2*, 331–335.

(40) Roversi, D.; Luca, V.; Aureli, S.; Park, Y.; Mangoni, M. L.; Stella, L. (2014) How Many Antimicrobial Peptide Molecules Kill a Bacterium? The Case of PMAP-23. *ACS Chem. Biol. 9*, 2003–2007. https://doi.org/10.1021/cb500426r.

(41) Futaki, S.; Suzuki, T.; Ohashi, W.; Yagami, T.; Tanaka, S.; Ueda, K.; Sugiura, Y. (2001) Arginine-Rich Peptides. An Abundant Source of Membrane-Permeable Peptides Having Potential as Carriers for Intracellular Protein Delivery. *J. Biol. Chem. 276*, 5836–5840. https://doi.org/10.1074/jbc.M007540200 M007540200 [pii].

(42) Eggimann, G. A.; Buschor, S.; Darbre, T.; Reymond, J. L. (2013) Convergent Synthesis and Cellular Uptake of Multivalent Cell Penetrating Peptides Derived from Tat, Antp, PVEC, TP10 and SAP. *Org. Biomol. Chem. 11*, 6717–6733. https://doi.org/10.1039/c3ob41023d.

(43) Nikaido, H. (1994) Prevention of Drug Access to Bacterial Targets: Permeability Barriers and Active Efflux. *Science 264*, 382–388. https://doi.org/10.1126/science.8153625.

(44) Iwasaki, A.; Medzhitov, R. (2004) Toll-like Receptor Control of the Adaptive Immune Responses. *Nat. Immunol. 5*, 987. https://doi.org/10.1038/ni1112.

(45) Opal, S. M. (2007) The Host Response to Endotoxin, Antilipopolysaccharide Strategies, and the Management of Severe Sepsis. *Int. J. Med. Microbiol. 297*, 365–377. https://doi.org/10.1016/j.ijmm.2007.03.006.

(46) Zughaier, S. M.; Shafer, W. M.; Stephens, D. S. (2005) Antimicrobial Peptides and Endotoxin Inhibit Cytokine and Nitric Oxide Release but Amplify Respiratory Burst Response in Human and Murine Macrophages. *Cell. Microbiol. 7*, 1251–1262. https://doi.org/10.1111/j.1462-5822.2005.00549.x.

(47) Tsuzuki, H.; Tani, T.; Ueyama, H.; Kodama, M. (2001) Lipopolysaccharide: Neutralization by Polymyxin B Shuts Down the Signaling Pathway of Nuclear Factor KB in Peripheral Blood Mononuclear Cells, Even during Activation. *J. Surg. Res. 100*, 127–134. https://doi.org/10.1006/jsre.2001.6227.

(48) Lindemann, R. A. (1988) Bacterial Activation of Human Natural Killer Cells: Role of Cell Surface Lipopolysaccharide. *Infect. Immun. 56*, 1301–1308.

(49) Domingues, M. M.; Inácio, R. G.; Raimundo, J. M.; Martins, M.; Castanho, M. A. R. B.; Santos, N. C. (2012) Biophysical Characterization of Polymyxin B Interaction with LPS Aggregates and Membrane Model Systems. *Biopolymers 98*, 338–344.

(50) Tada, R.; Koide, Y.; Yamamuro, M.; Hidaka, A.; Nagao, K.; Negishi, Y.; Aramaki, Y. (2013) Maleylated-BSA Induces TNF-α Production through the ERK and NF-KB Signaling Pathways in Murine RAW264.7 Macrophages. *Open. J. Immunol. 2013*. https://doi.org/10.4236/oji.2013.34023.

(51) Lu, X.-X.; Jiang, Y.-F.; Li, H.; Ou, Y.-Y.; Zhang, Z.-D.; Di, H.-Y.; Chen, D.-F.; Zhang, Y.-Y. (2017) Polymyxin B as an Inhibitor of Lipopolysaccharides Contamination of Herb Crude Polysaccharides in Mononuclear Cells. *Chin. J. Nat. Med. 15*, 487–494. https://doi.org/10.1016/S1875-5364(17)30074-2.

(52) Adams, P. G.; Lamoureux, L.; Swingle, K. L.; Mukundan, H.; Montaño, G. A. (2014) Lipopolysaccharide-Induced Dynamic Lipid Membrane Reorganization: Tubules, Perforations, and Stacks. *Biophys. J. 106*, 2395–2407. https://doi.org/10.1016/j.bpj.2014.04.016.

(53) Tam, V. H.; Schilling, A. N.; Vo, G.; Kabbara, S.; Kwa, A. L.; Wiederhold, N. P.; Lewis, R. E. (2005) Pharmacodynamics of Polymyxin B against Pseudomonas Aeruginosa. *Antimicrob. Agents Chemother. 49*, 3624–3630. https://doi.org/10.1128/AAC.49.9.3624-3630.2005.

(54) Lv, Y.; Wang, J.; Gao, H.; Wang, Z.; Dong, N.; Ma, Q.; Shan, A. (2014) Antimicrobial Properties and Membrane-Active Mechanism of a Potential α-Helical Antimicrobial Derived from Cathelicidin PMAP-36. *PLOS ONE 9*, e86364. https://doi.org/10.1371/journal.pone.0086364.

For Table of Contents Use Only: